Int J Adv Manuf Technol (2018) 94:4065–4071
DOI 10.1007/s00170-017-1114-3

ORIGINAL ARTICLE

Investigation on critical cutting depth in milling of wave-transmitting Si_3N_4 ceramics

Yunfeng Liu [1] · Xianli Liu [1] · Shiliang Wei [1] · Hong Zhao [2]

Received: 17 May 2017 / Accepted: 13 September 2017 / Published online: 27 September 2017

Abstract Wave-transmitting Si_3N_4 ceramics exhibits high levels of brittleness, and the milling surface inevitably exists defects. Critical cutting depth is an important reference parameter to improve the surface quality and processing efficiency in milling. A theoretical mathematical model has been proposed to predict the critical cutting depth in the study. The contact relationship between the tool cutting edge and the ceramics surface is analyzed, and the non-uniform bearing crack system is established. The micro cracks propagation critical condition has been put as the criterion of critical cutting depth. Through the model calculation, the critical cutting depth is 0.38 mm, and it is confirmed the critical cutting depth is between 0.3 and 0.4 mm with experimental results. The model predictions are consistent well with the experimental results. In addition, the theoretical model shows that the critical cutting depth decreases exponentially with the increase of the material hardness, while the increase of fracture toughness, tool helix angle and side edge rear angle, leads to critical cutting depth rising. The theoretical model can be applied to evaluate the critical cutting depth of brittle ceramics in milling.

Keywords Critical cutting depth · Theoretical model · Wave-transmitting Si_3N_4 ceramics · Milling

✉ Shiliang Wei
weishiliang@hrbeu.edu.cn

[1] Mechanical & Power Engineering College, Harbin University of Science and Technology, Harbin 154001, People's Republic of China

[2] College of Mechanical and Electronic Engineering, Harbin Engineering University, Harbin 154001, People's Republic of China

1 Introduction

Wave-transmitting Si_3N_4 ceramics has been applied in aerospace field widely due to superior comprehensive mechanical properties and dielectric loss [1]. Compared with other engineering ceramics, the hardness of wave-transmitting Si_3N_4 ceramics is lower, so its parts can be realized in milling, instead of grinding or rotary ultrasonic grinding. However, the low fracture toughness is still the inherent characteristic, and its fracture toughness value is less than 3 MPa $m^{1/2}$. The milling surface inevitably exists pits, collapse, and other defects. Wave-transmitting Si_3N_4 ceramics material is mainly made into antenna window, used in missiles and hypersonic vehicles. These surface defects are important factors affecting the service life and reliability of parts. In order to improve the surface quality, it is necessary to study brittle ceramics milling technology.

Compared with brittle ceramics milling, more investigations are focused on brittle ceramics grinding technology. Li et al. studied the removal mechanism of nano-ZrO_2 ceramics in grinding, and the results show that the removal mechanism changes as the cutting depth increases [2]. Fang et al. have proved that there are plastic flow and brittle fracture materials in hard and brittle materials machining [3]. Lv et al. have studied the rotary ultrasonic grinding of BK7 glass; it is concluded that the surface appears brittle and plastic transition, and gradually, small cracks generate with the increase of the cutting depth [4, 5]. They proved that material removal mechanism of rotary ultrasonic grinding is mainly brittle fracture. Nath et al. found that there are lateral and longitudinal cracks in the ceramics surface with the tool abrasive action for rotary ultrasonic grinding [6]. They also draw conclusions that the lateral cracks is the main mechanism of material removal and longitudinal cracks is the main mechanism of surface defects formation.

Due to the low fracture toughness of ceramics, no matter what kind of machining methods, material removal patterns include plastic removal and brittle removal [7, 8]. Rusnaldy et al. studied monocrystalline silicon milling, used diamond-coated tools, and realized the ductile domain milling at depth of 0.3 μm. As the cutting depth increases, the machined surface gradually appears the brittle fracture area, forming large-scale damage surface, and chips of varying sizes and irregular shapes [9]. Liu et al. pointed out that when the tool has a large negative angle, it is easy to form the compressive stress region in the cutting zone and inhibit the expansion of micro cracks [10]. Zhou et al. studied the mechanism of chip formation in brittle ceramics high-speed milling and presented that brittle ceramics chips are mainly composed of extruded particles and broken crusts, so the machined surfaces are full of pits [11]. Zuo et al. suggested that there is critical depth of fully sintered zirconia in milling to achieve ductile milling, and it has been proved with experimental results [12]. The same conclusions were also obtained [13].

There are plastic removal and brittleness removal of ceramics materials in milling, but there is no effective method for critical cutting depth determination except experiments. Critical cutting depth is an important reference parameter to improve the surface quality and processing efficiency in milling. In this paper, wave-transmitting Si_3N_4 ceramics in milling will be investigated. The tool-workpiece contact relation will be conducted, and a theoretical model based on the tip stress field intensity of the non-uniform bearing cracks system is developed to predict the critical cutting depth. Finally, experiments will be designed to verify the model.

2 The model of critical cutting depth in milling

Figure 1 shows the plane milling of wave-transmitting Si_3N_4 ceramics. The cutting edge of the tool is in discontinuous contact with the material removal side. Section views the contact area of tool and ceramics material paralleling to the XOY surface and XOZ plane, respectively; the relationships between the tool cutting edge and the ceramics are shown as Fig. 1b, c. Figure 1b is the horizontal direction view and Fig. 1c is the vertical direction view. Where λ_o is the tool front angle, β is the tool helix angle, α_0 is tool side edge rear angle, and h is the milling depth.

Milling depth direction parallels to the XOZ plane. In order to analyze the critical cutting depth, only the contact relationship between tool and material in Fig. 1c is conducted. Through the coordinate transformation, the XOZ coordinate is turned to $X'OZ'$, so the tool cutting edge and the material surface contact are shown in Fig. 2.

In the coordinate of $X'OZ'$, the horizontal concentrated load force called F_t and the vertical concentrated load force called F_n are produced under the effect of cutting force F_x and F_z. The contact problem between the cutting edge and the material surface can be simulated as the isotropic elastic semi-infinite body internal stress distribution under the action of the horizontal force and the tangential force. It is the Boussinesq field and the Cerruti field. So the stress distribution of the ceramics material can be expressed as follows:

$$\begin{cases} \sigma_{x'} = \dfrac{F_n}{2\pi R^2}\left\{(1-2\mu)\left[\dfrac{z'}{R}-\dfrac{R}{R+z'}+\dfrac{x'^2(2R+z')}{R(R+z')^2}\right]-\dfrac{3x'^2z'}{R^3}\right\} \\ \sigma_{z'} = -\dfrac{3F_n z'^3}{2\pi R^5} \end{cases} \tag{1}$$

$$\begin{cases} \sigma_{x'} = \dfrac{F_t x'}{2\pi R^3}\left[\dfrac{(1-2\mu)R^2}{(R+z')^2}-\dfrac{3x'^2}{R^2}\right] \\ \sigma_{z'} = -\dfrac{3F_t x' z'^2}{2\pi R^5} \end{cases} \tag{2}$$

Where μ is Poisson ratio of ceramics. The tool cutting edge can be simplified as a sharp conical indenter, and the corner angle is expressed as Eq. (3).

$$\theta = 0.5(\pi/2-\beta-\lambda_o) \tag{3}$$

In the coordinate of $X'OZ'$, for the contact line of the cutting edge and material surface, the relationship between x' and z' can be described as follows:

$$x' = \tan\theta\left(c-z'\right) \tag{4}$$

Where c is press depth of the cutting edge.

So the distance is obtained by the following equation.

$$R = \sqrt{x'^2+z'^2} = \sqrt{\tan^2\theta(c-z')^2+z'^2} \tag{5}$$

There is a friction coefficient called η to describe the level of horizontal concentrated force and the vertical concentrated load force, and the vertical concentrated load force can be derived as follows:

$$F_t = \eta F_n \tag{6}$$

According to the coordinate transformation angle relationship, the friction coefficient called η can be calculated as Eq. (5) with the cutting force F_x and F_z.

$$\eta = \frac{F_x\cos(\theta+\lambda_0)+F_z\sin(\theta+\beta)}{F_x\sin(\theta+\lambda_0)-F_z\cos(\theta+\beta)} \tag{7}$$

The tool cutting edge is simplified as a sharp tapered indenter, which is pressed into the ceramics surface under the applied vertical load to causing the plastic deformation. The relationship between the vertical load and the surface indentation feature size and material hardness can be expressed as follows:

$$F_n = \alpha\pi(c\cdot\tan\theta)^2 H \tag{8}$$

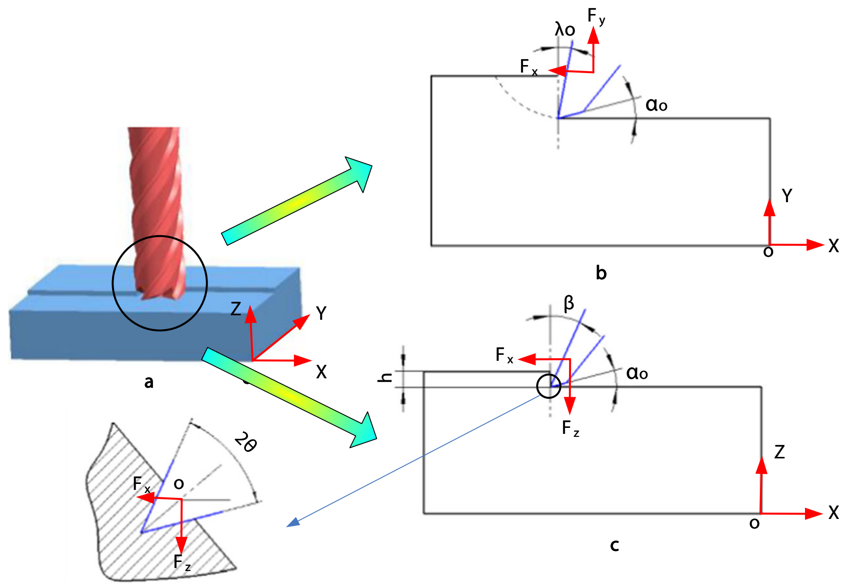

Fig. 1 Plane milling of wave-transmitting Si_3N_4 ceramics

Where α is the indenter shape factor, generally is equal to $\pi/2$.

Under the common action of horizontal concentrated force and the vertical concentrated force, the stress of X' direction in the ceramics can be described as follows:

$$\sigma_{x'}\left(z'\right) = \frac{F_n}{2\pi R^2}\left[\frac{(1-2\mu)R}{R+z'} - \frac{3x'^2 z'}{R^3}\right] + \frac{F_t x'}{2\pi R^2}\left[\frac{(1-2\mu)R^2}{(R+z')^2} - \frac{3x'^2}{R^2}\right] \quad (9)$$

It can be seen that the contact surface stress distribution between the cutting edge and the material is typical non-uniform bearing system. The cutting edge pressed into the material interior can be assumed to be a preset single-pass micro crack. So the system is assumed to be non-uniform bearing crack system. Then the tip stress intensity of the cutting edge can be obtained as follows:

$$K_I = 2m\sqrt{\frac{c}{\pi}}\int_0^c \frac{\sigma_{x'}\left(z'\right)}{\sqrt{c^2 - z'^2}}dz \quad (10)$$

Where m is correction factor and about equal to 1.12.

When the cutting depth is less than the critical cutting depth, the material removal process is plastic removal, and the machined surface has no micro cracks. Then the tip stress intensity of cutting edge must be less than the fracture toughness value called K_{Ic} of ceramic material. If $K_I = K_{Ic}$, the critical press depth of the cutting edge can be obtained by Eq. (10), and the critical cutting depth can be derived as follows:

$$h^* = \frac{c^* \cdot \cos\beta}{\cos\theta} \quad (11)$$

3 Experimental design

To verify the model reliability of critical cutting depth and analyze the influence of cutting depth, the wave-transmitting Si_3N_4 ceramics milling experiments have been designed. The wave-transmitting Si_3N_4 ceramics is homogeneous, and the

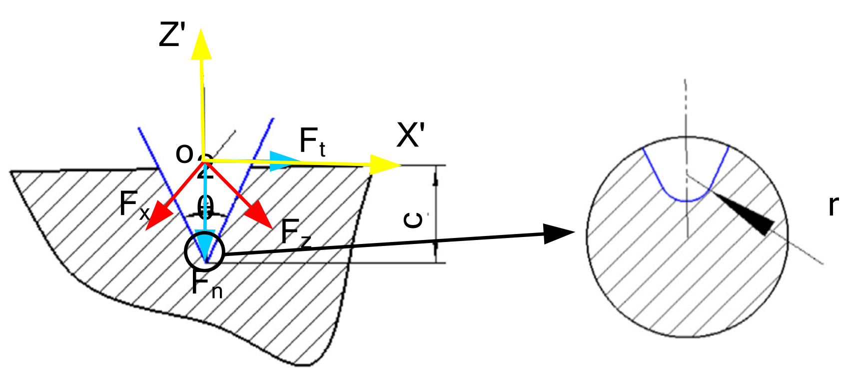

Fig. 2 Tool cutting edge and the material surface contact

Table 1 Main parameters of the material

Parameters Material	Elasticity modulus (GPa)	Hardness (MPa)	Fracture toughness ($MPa{\cdot}m^{1/2}$)	Density ($g{\cdot}cm^3$)
Si_3N_4	104	210	2.6	1.9

size of samples is 40 × 40 × 10 mm. The main material properties parameters are listed in Table 1.

The experiments were conducted on JDGR200_A10H CNC milling machine. The cutting tools used in the experiments are cemented carbide end mills. The parameters is that the number of blades is 4, the front angle is 8°, the rear angle is 10°, and the helix angle is 30°. Single test design is used to arrange experimental parameters, and the experimental no. is 8. Table 2 shows the program.

The wave-transmitting Si_3N_4 ceramics samples were machined by milling, shown as Fig. 3, with machining width 1 mm, according to the experimental sequence and parameters. The cutting forces were measured by KISTLER 9257A dynamometer and KISTLER 5070 charge amplifier. The machined surface of each sample was observed by VHX-1000 depth of field microscopy and OLS3000 confocal scanning laser microscope. The chip has been collected and observed by FEI HELIOS NanoLab 600I FIB/SEM double beam system.

4 Results discussion

4.1 Experimental analysis of different cutting depth

As the cutting depth increases from 0.1 to 0.8 mm, the cutting force curves are shown in Fig. 4. The cutting force change trend of X, Y, and Z direction is presented increasing firstly, then declining, and finally increasing. For wave-transmitting Si_3N_4 ceramics in milling, if the removal mechanism is the same, the cutting force will rise with the increase of cutting depth. However, when the cutting depth is between 0.3 and 0.4 mm, the cutting force is abruptly changed, indicating that the material removal mechanism has changed from plastic removal to brittle removal, resulting in reduced cutting force. Therefore, the critical cutting depth is considered to be greater than 0.3 mm and less than 0.4 mm.

Table 2 Experimental program

Experimental number	Speed (r/min)	Cutting depth (mm)	Feed rate (mm/min)
1	3200	0.1	400
2	3200	0.2	400
3	3200	0.3	400
4	3200	0.4	400
5	3200	0.5	400
6	3200	0.6	400
7	3200	0.7	400
8	3200	0.8	400

To prove this conclusion furtherly, the surface of the wave-transmitting Si_3N_4 ceramics in milling has been analyzed. Figure 5 shows the variation of the surface arithmetic mean deviation called Sa and the surface root mean square deviation called Sq under different cutting depth parameters. When the cutting depth is between 0.3 and 0.4 mm, the surface roughness also decreases and mutations have occurred.

Figure 6 presents the chip morphology of different cutting depths. When the cutting depth is 0.1, 0.2, and 0.3 mm, the chip of wave-transmitting Si_3N_4 ceramics is mainly material powder, and its shape is more rough. So the material removal mechanism is plastic removal. However, when the cutting depth is 0.4 mm, in addition to material powder, a large number of fragmented particles appear in the chip. The difference from the cluster powder is that the surface morphology is smoother. Fragmented particles are produced due to the peeling off of material in milling that is brittle removal. And when the cutting depth is greater than 0.4 mm, fragmentation particles in the chip are more and more obvious.

It is worth noting that during the brittle removal process, under the action of large cutting force, the crack propagation length and the removal rate of the adjacent crack propagation material are larger, resulting in the surface after the material removal is relatively gentle. So the surface roughness downs,

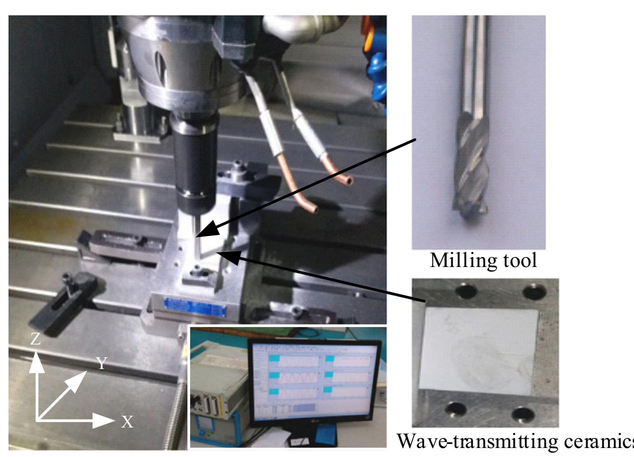

Fig. 3 Experimental setup

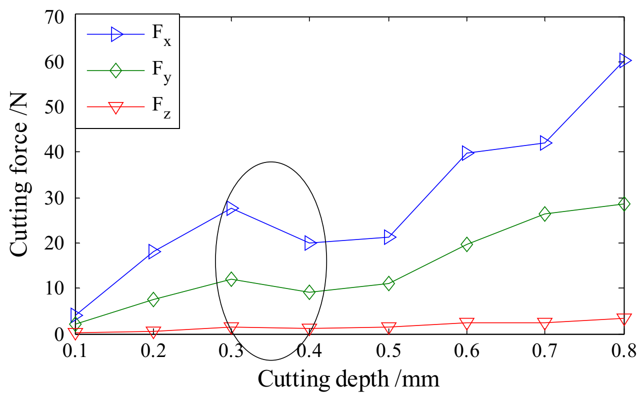

Fig. 4 Cutting force curves

as shown in Fig. 5 when the cutting depth is between 0.6 and 0.7 mm.

Figure 7 shows the machined surface topography obtained when the cutting depth is 0.3 and 0.4 mm, respectively. The ups and downs of surface morphology is uniform, the density is great, there are no obvious pits, nothing is broken, and no other machining defects, as the cutting depth is 0.3 mm. However, the volume of surface convex and concave peak increases, and the machining defects such as pits and pits occur, as the cutting depth is 0.4 mm. The formation of these surface machining defects is closely related to the propagation of micro cracks in the machined surface. When the cutting depth is 0.4 mm, the material removal mechanism is brittle removal.

The change of the material removal mechanism is also manifested in the surface edge chipping. Figure 8 shows the edge chipping patterns obtained when the depth of cut is 0.3 and 0.4 mm, respectively. When the cutting depth is 0.3 mm, the surface edge of the wave-transmitting Si_3N_4 ceramics is not damaged. But when the cutting depth is 0.4 mm, the surface edge is damaged and the edge is broken.

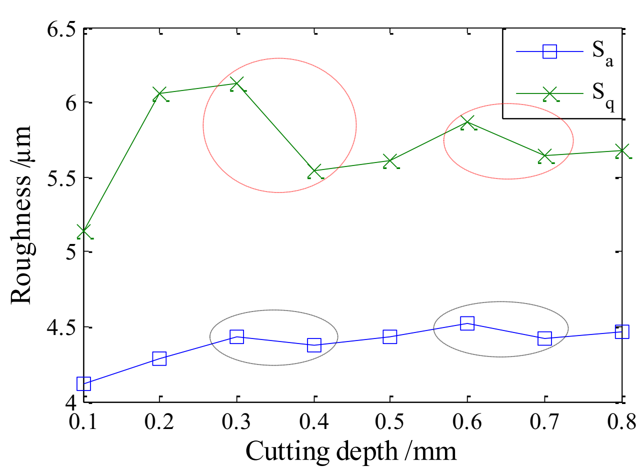

Fig. 5 Roughness of under different cutting depth

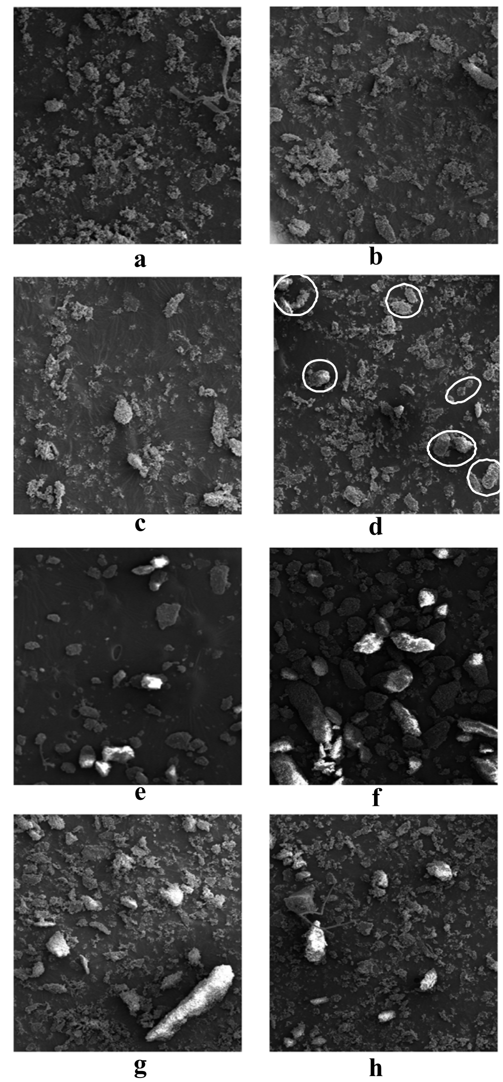

Fig. 6 Chip morphology of different cutting depth. **a** 0.1 mm. **b** 0.2 mm. **c** 0.3 mm. **d** 0.4 mm. **e** 0.5 mm. **f** 0.6 mm. **g** 0.7 mm. **h** 0.8 mm

From the analysis of the above experimental results, it is concluded that when the cutting depth is less than or equal to 0.3 mm, the material removal mechanism is plastic removal. When the cutting depth is 0.4 mm or more, the material removal method is brittle removal, so the critical cutting depth of the wave-transmitting Si_3N_4 ceramics in milling should be between 0.3 and 0.4 mm.

4.2 Critical cutting depth model validation and change

When the cutting depth is 0.1, 0.2, and 0.3 mm, the material removal mechanism is plastic removal. According to the experimental value of the cutting force and Eq. (6), it can be got that $\eta \approx 1$.

The material parameters, tool parameters, and experimental results are brought into Eq. (10). If $K_I = K_{Ic}$, then it is found that the critical cutting depth of wave- transmitting Si_3N_4

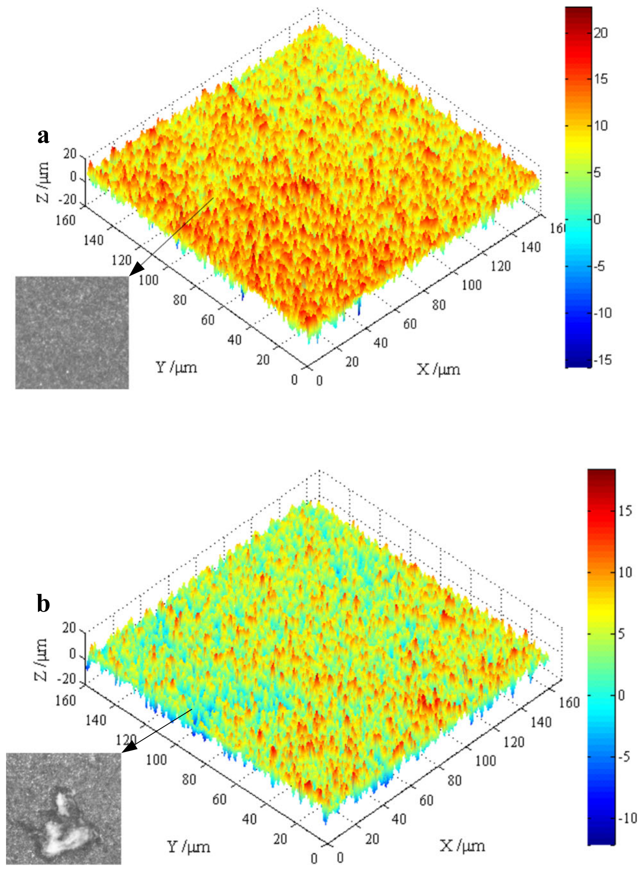

Fig. 7 Surface morphology of different cutting depth. **a** 0.3 mm. **b** 0.4 mm

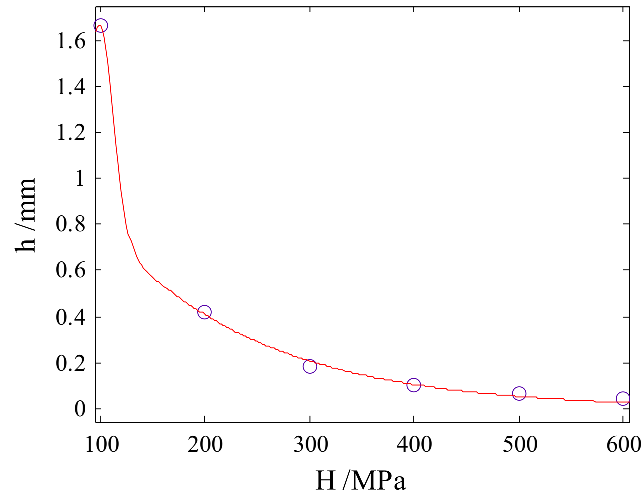

Fig. 9 Effect of material hardness on critical cutting depth

ceramics in milling is 0.38 mm. The experimental results show the critical cutting depth is between 0.3 and 0.4 mm. The theoretical calculation results are in good agreement with the experimental results, which proves that the critical cutting depth calculation model of wave-transmitting Si_3N_4 ceramics is reasonable.

According to the critical cutting depth calculation model, the relationship between critical cutting depth and influencing factors can be studied. Figure 9 shows the effect of material hardness on critical cutting depth. With the hardness increasing, the critical cutting depth decreases exponentially. The effect of the hardness on the cutting force is the most significant. The increased hardness will lead to the cutting force adding, and it causes the stress at the tip of the cutting edge ascension. If the fracture toughness of the ceramics material is constant, the critical cutting depth decreases inevitably.

Figure 10 shows the effect of material fracture toughness on critical cutting depth. The fracture toughness has significant effect on the critical cutting depth. With the increase of the fracture toughness, the critical cutting depth is increased by the second term. As the fracture toughness increases, the elastic-plastic deformation ability of the material is improved, and the brittle fracture is more difficult to occur in milling, which leads to the critical cutting depth rising.

In addition to the performance of the ceramics material, the milling tool parameters are also important factors affecting the critical cutting depth. Figure 11 shows the effect of the tool helix angle and the tool side edge rear angle on the critical cutting depth. The helix angle and the rear angle increase, resulting in the corner angle of the cutting edge decreases. With the same load, the depth pressure into the material adds, resulting in increased critical cutting depth. Therefore, in order to improve the critical cutting depth, the helix angle and the rear angle can be appropriately raised. But the increased helix

Fig. 8 Edge chipping of different cutting depth. **a** 0.3 mm. **b** 0.4 mm

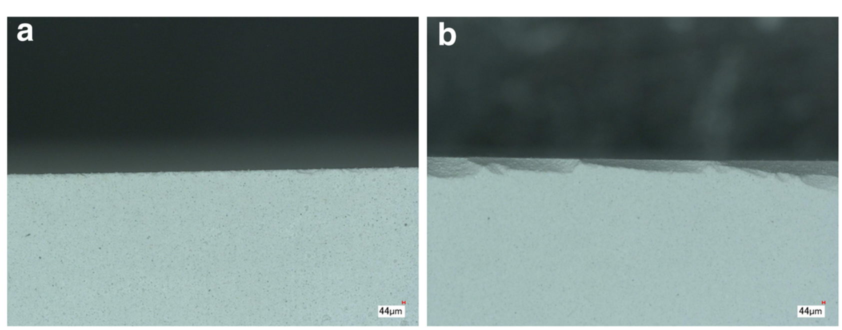

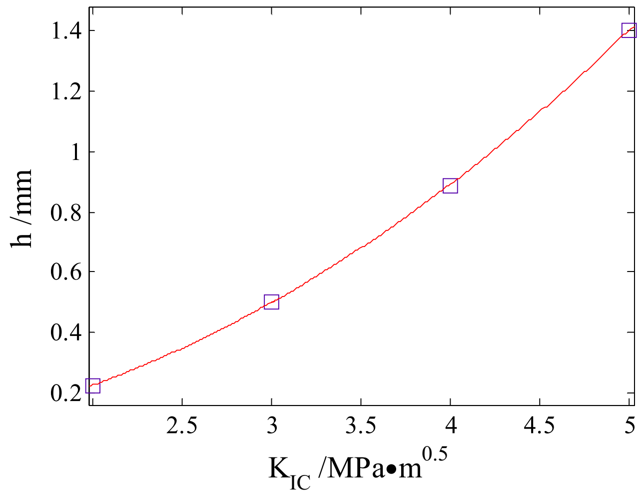

Fig. 10 Effect of fracture toughness on critical cutting depth

angle and rear angle lead to the sharpening of the cutting edge, and the tool wear is more serious.

5 Conclusions

A theoretical critical cutting depth of wave-transmitting Si_3N_4 ceramics in milling has been developed. The following conclusions can be summarized from the study:

Micro cracks propagation critical condition is the criterion of critical cutting depth. The cutting edge is pressed into the interior of the material surface; its stress field is combined by the Boussinesq field and the Cerruti field, and the non-uniform bearing crack system is formed. By solving the stress field intensity of the cutting edge tip, critical cutting depth calculation model has been established.

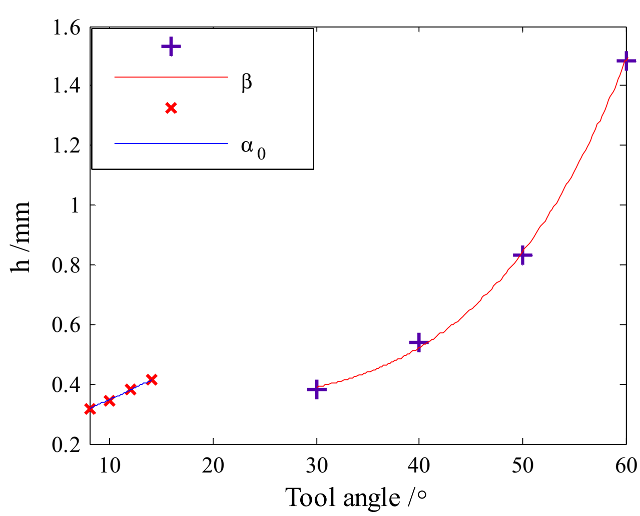

Fig. 11 Effect of tool angles on critical cutting depth

As the cutting depth is between 0.3 and 0.4 mm, the cutting force and surface roughness are abruptly changed. It is further confirmed that when the cutting depth is 0.3 mm, the chip is consist of the material powder, and the machining surface has no defects, and when the cutting depth is 0.4 mm, broken ceramics particles appear, and the machining surface contains defects. Thus, it is confirmed the critical cutting depth should be between 0.3 and 0.4 mm.

The critical cutting depth is 0.38 mm with calculation model, which is consistent with the experimental results. It is proved that the model is reasonable. The critical cutting depth decreases exponentially with the increase of the material hardness, while the increase of fracture toughness, tool helix angle and side edge rear angle, leads to critical cutting depth rising.

Funding information The authors would like to thank China Postdoctoral Science Foundation funded project under No. 2015M581462.

References

1. Chen M, Yin XW, Li M, Chen LQ (2015) Electromagnetic interference shielding properties of silicon nitride ceramics reinforced by in situ grown carbon nanotubes. Ceram Int 41(2):2467–2475
2. Han ZL, Li CH, Wang S, Mao WP (2013) Experimental investigation into material removal mechanism of Nano-ZrO_2 dental ceramic grinding. China Mech Eng 24(09):1150–1154
3. Fang FZ, Zhang GX (2004) An experimental study of optical glass machining. Int J Adv Manuf Technol 23(3–4):55–160
4. Lv DW, Hong X, Tang YJ, Huang YH, Li ZP (2013) Influences of vibration on surface formation in rotary ultrasonic machining of glass BK7. Precis Eng 37(4):839–848
5. Lv DW, Huang YH, Wang H (2013) Improvement effects of vibration on cutting force in rotary ultrasonic machining of BK7 glass. J Mater Process Technol 213(9):1548–1557
6. Nath C, Lim GC, Zheng HY (2011) Influence of the material removal mechanisms on hole integrity in ultrasonic machining of structural ceramics. Ultrasonics 52(5):605–613
7. Qin N, Pei ZJ, Treadwell C, Guo DM (2009) Physics-based predictive cutting force model in ultrasonic-vibration-assisted grinding for titanium drilling. J Manuf Sci Eng Trans ASME 131(4):0410111–0410119
8. Ya G, Qin WH, Yang SC, Xu YW (2002) Analysis of the rotary ultrasonic machining mechanism. J Mater Process Technol 129(1–3):182–185
9. Rusnaldy TJK, Kim HS (2007) Micro-end-milling of single-crystal silicon. Int J Mach Tools Manuf 47(14):2111–2119
10. Liu K, Li X, Liang S (2007) The mechanism of ductile chip formation in cutting of brittle materials. Int J Adv Manuf Technol 33(9):875–884
11. Wang CY, Zhou L, Fu H, Hu ZL (2007) High speed milling of graphite electrode with endmill of small diameter. Chin J Mech Eng 20(4):27–31P
12. Wu H, Zuo DW, Sun QP, Sun YL (2015) Research on ductile regime milling of fully sintered dental zirconia. Trans Beijing Inst Technol 35(9):902–907
13. Bian R, He N, Ding WZ, Liu SQ (2017) A study on the tool wear of PCD micro end mills in ductile milling of ZrO_2 ceramics. Int J Adv Manuf Technol 2017:1–10